Scanning electrochemical microscopy for the investigation of corrosion processes: measurement of Zn^{2+} spatial distribution with ion selective microelectrodes

Javier Izquierdo[a], Lívia Nagy[b], Ágnes Varga[b], István Bitter[c], Géza Nagy[b], Ricardo M. Souto[a,d]

[a] Department of Physical Chemistry, University of La Laguna, E-38200 La Laguna, Tenerife, Canary Islands, Spain

[b] Department of General and Physical Chemistry, Faculty of Sciences, University of Pécs, 7624 Pécs, Ifjúság útja 6, Hungary

[c] Budapest University of Technology and Economics, Budafoki u. 8, 1111 Budapest, Hungary

[d] Instituto Universitario de Materiales y Nanotecnologías, University of La Laguna, E-38200 La Laguna, Tenerife, Canary Islands, Spain

Abstract

Ion-selective microelectrodes can be employed as tips in scanning electrochemical microscopy (SECM) for chemical imaging of corrosion processes. They present higher chemical selectivity than conventional amperometric microdisks, and may be the only effective option to visualize the dissolution of metals with negative redox potentials in aqueous environments when the use of Pt microelectrodes is limited by the onset of oxygen reduction and hydrogen evolution reactions. A robust micro-sized ion selective electrode has been developed which allows the spatial distribution of Zn^{2+} during galvanic corrosion of a model Fe/Zn couple to be investigated using SECM. Owing to the low internal contact potential and smaller membrane thickness achieved with the novel design, the resistance of the micropipette electrodes is only fractions of the resistance of conventional micropipette electrodes of the same size. As a result, no special shielding of the microelectrodes is required and higher scanning rate can be used for scanning in the potentiometric modes using these micropipette tips. Concentration profiles over corroding surfaces measured with this technique will be presented.

Keywords: scanning electrochemical microscopy; potentiometric operation; ion selective microelectrode; zinc; galvanic corrosion.

1. Introduction

Scanning electrochemical microscopy (SECM) has become a powerful technique for studying the complex processes involved in Corrosion Science due to its ability to image the topography and to probe chemical reactivity in micrometer- and submicrometer-sized dimensions [1-4]. The use of an ultramicroelectrode (UME) that is scanned across the surface of a sample, allows interfaces to be characterized with spatial resolution whereas almost any kind of electrochemical measurement can be performed at the SECM tip and at the substrate surface. To date, SECM has found application in the detection of precursor sites [5-7] and the visualization of metastable regime [8] for pitting corrosion, the characterization of the chemical stability of thin surface films [9-12] and organic coatings applied on metals [13-26], the detection of metal and inclusion dissolution [25-27], the recognition of anodic and cathodic areas [28,29], hydrogen permeation [30], etc. These studies have supplied valuable information using metal microdisks as the tip, and amperometric operation of the SECM. That electrochemical information is derived from the measurement of the faradaic current flowing through the ultramicroelectrode tip as a function of either time or its position above the sample. Yet, limited application of this technique occurs when more than one chemical species can simultaneously react at the microdisk tip, thus compromising chemical selectivity [31], and when the species sensed at the tip reacts with it, giving rise to changes in the surface condition and composition of the material. Thus, there is need for new techniques and procedures in SECM that may provide greater selectivity for chemical imaging of corrosion processes.

Scanning electrochemical microscopy can also be operated in a potentiometric mode by employing an ion-selective microelectrode (ISME) as the tip [32-35]. They present higher chemical selectivity than conventional amperometric microdisks, and may be the only effective option to visualize the dissolution of metals with negative redox potentials in aqueous environments when the use of Pt microelectrodes is limited by the onset of oxygen reduction and hydrogen evolution reactions [36,37]. However a quick survey of the scientific literature concerning the use of SECM, serves to observe that the potentiometric method has been applied rather scarcely compared to conventional amperometric modes. The reason for this situation arises from the very high resistance and limited stability exhibited by the ISMEs, which require careful shielding of the electrochemical cell and very slow scanning rates. The resistance value in an ISME arises from the relatively thick organic cocktail layer and liquid contact between the ionophore containing cocktail and the filling solution of the inner reference. This is the reason that the potentiometric SECM has been almost

completely limited to pH monitoring by using solid state microelectrodes based on the characteristics of certain oxides of transition metals, or solid state chloride electrode [32,38-40]

The situation has greatly changed due to the development of robust micro-sized ion selective electrode containing a solid contact between the ionophore and the inner reference solution [41,42]. Owing to the low internal contact potential and smaller membrane thickness achieved with the novel design, the resistance of the micropipette electrodes are only fractions of the resistance of conventional micropipette electrodes of the same size. As a result, no special shielding of the microelectrodes is required and higher scanning rate can be employed in the potentiometric mode using micropipette tips. Very recently, the fabrication of a solid contact micropipette ion selective microelectrode for Zn^{2+} ions has been reported [43]. Since zinc is a metal widely employed in our technological society, the corrosion of this metal in aqueous environments has been extensively investigated up to now. In particular, the role of corrosion products to inhibit the cathodic reaction and the possibility of additional self-healing effects for corrosion protection due to additives in the composition of the metal alloy or arising from surface treatments, are a hot research topic in the case of galvanized steels. To understand the role of corrosion products of galvanized steels, it is necessary to measure the concentration distributions of Zn^{2+} and OH^- ions in the solution above the surface. Whereas pH monitoring is already available using the SECM [38-40], the measurement of the distribution of the metal ions was not possible with this technique until now.

The present study investigated the applicability of a solid contact Zn^{2+}-ISME to measure the spatial concentration distribution of dissolved zinc over corroding surfaces measured with SECM operated in potentiometric mode

2. Experimental

2.1. Samples

The substrate consisted of 99.5% purity iron and 99.95% purity zinc surfaces mounted into an epoxy resin sleeve, such that only an 1 x 1 mm^2 square end surface formed the testing metal substrates. These metals were supplied as sheets of thickness 1 mm by Goodfellow Materials Ltd. (Cambridge, UK). The front side of the mounts was grinded with silicon carbide paper down to 4000 grit, and followed by a polishing step with 0.3 μm alumina slurries. Samples were then washed thoroughly with

ultra-pure deionized water and allowed to dry in air. The corrosive medium was 10 mM NaCl solution in contact with air, quiescent and at ambient temperature.

2.2. Zn^{2+}-ion selective microelectrodes

The ion selective cocktail was prepared using was N-phenyliminodiacetic acid bis-N',N'-dicyclohexylamide as zinc ionophore, potassium tetrakis(4-chlorophenyl)borate (KTCPB), 2-nitrophenyl octhyl ether (NPOE) and PVC in tetrahydrofurane (THF). The composition of the mixture was: 57.7 wt.% NPOE, 3.6 wt.% Zn ionophore, 3.4 wt.% PVC, 1.3 wt.% KTCPB, and 34.0 wt.% THF. The synthesis of N-phenyliminodiacetic acid bis-N',N'-dicyclohexylamide zinc ionophore can be found in ref. [44].

Two different kinds of zinc-ion selective microelectrodes were prepared using micropipettes pulled from acid washed, and dried borosilicate glass capillaries (B100-50-10 and B200-116-10; Sutter Instruments, Novato, CA, USA), namely solid contact and conventional microelectrodes. The conventional micropipette ion selective electrodes were fabricated according to the established methodology [45,46], whereas the solid contact ion-selective microelectrodes were manufactured with the new procedure described in refs. [41,43]. In brief, these novel micropipette electrodes were made of two parts as shown in Figure 1A. Two micropipettes were pulled from glass capillaries using a pipette puller, and subsequently silanized by introducing inside their tip a few microliters of 5% dimethyldichlorosilane solution in carbon tetrachloride. The hydrophobic layer was completed after heating the pipettes at 80 °C in an oven for about 30 min. The cocktail was backfilled into the tip through a very thin glass capillary attached to the syringe needle used. The internal solid contact is provided by a PEDOT-coated carbon fibre of 33 μm diameter (obtained as a generous gift from Specialty Materials, Lowell, Massachusetts, USA) dipped in the cocktail. Conventional micropipette electrodes used an internal filling solution (0.25 M potassium chloride containing 10 mM $ZnCl_2$) in contact with the cocktail and a chloride coated silver wire introduced as internal reference electrode as depicted in Figure 1B.

2.3. Instrumentation

The SECM instrument has been described previously [47]. Main components are a 3D positioning stage driven by stepper motors (MFN 25PP; Newport, Irvine, CA, USA), a battery-powered voltage follower based on an operational amplifier (TL082; National Semiconductor, Santa Clara, CA; USA), a digital multimeter (M-3630D; METEX, Seoul, Korea) and home-built control software. A video camera was used to

4

further assist positioning of the tip close to the surface. The electrochemical cell was composed by the ISME as tip, and an Ag/AgCl/3 M KCl as reference electrode.

3. Results and discussion

3.1. Characterization of the Zn^{2+}-ion selective electrodes

We were primarily concerned with the fabrication of zinc ion selective microelectrodes for SECM operation. The calibration procedure consisted in the introduction of the microelectrode in a sequence of $ZnSO_4$ solutions with 10^{-x} molar concentration, with $-6 \leq x \leq -1$. The procedure was initiated with the most diluted solution and subsequently exposed to solutions of increased concentration. After a brief period overpotential values occurring upon electrolyte exchange, the electrode always attained a steady potential value in each solution. With the potential values taken from each solution, the calibration plot shown in Figure 2 was drawn. It can be observed that there is a linear relationship between the potential of the ISME and the minus logarithm of concentration of zinc ions, and the slope of the plot is 29.8 mV/decade. The activity coefficients were calculated using the Debye-Hückel approximation.

3.2. Potentiometric SECM

The performance of the solid contact Zn^{2+}-ISME to image metal ion concentrations originating from a corroding surface using SECM was explored on a zinc-iron galvanic pair exposed to a 10 mM NaCl aqueous solution, open to air and at ambient temperature. Figure 3A depicts SECM scan lines obtained above the zinc specimen for different exposure times ranging from 1 to 177 minutes. That is, the ISME tip is moved in the X direction at a constant vertical distance of 25 μm from the substrate, starting from a position on the resin sleeve close to the zinc squared strip. Indeed, the scanning probe rasters the zinc surface for $1020 < X < 2260$ μm, and subsequently continues its movement on the epoxy sleeve in direction towards the location of the iron sample. The tip movement was stopped before reaching the iron surface in this case, though a sufficiently long excursion above the insulating resin was made as to allow the probe to travel in a portion of the electrolyte with a concentration distribution characteristic of the bulk electrolyte. All the line scans were taken on the same line passing through the center of both metal samples, in order to unambiguously monitor changes related to the advancement of the corrosion process. The onset of

galvanic corrosion leads to the oxidation of zinc with the release of Zn^{2+} ions, whereas the cathodic process is located on the iron surface (not shown in the figure).

The first scan line recorded just after the electrolyte was added to the cell container and the chosen probe-substrate distance was attained, closely describes the initial conditions of the system. The potential recorded at the ISME shows an almost constant reading below the lower limit of detection of the microelectrode as from the calibration curve in Figure 2), regardless the probe travelling above either the zinc strip or the insulating resin. This condition is described in the graph by pZn values close to 7. Yet, a more detailed inspection of the plot corresponding to this initial condition does exhibit some trends consistent with the dynamics of the corroding system. The pZn values show a tendency to decrease from left to right while the probe is passing above the zinc strip. Though zinc concentrations are below the range for their quantitative determination, the progress of the corrosion reaction and the subsequent release of Zn^{2+} ions, leads to the probe travelling into positions of greater metal concentrations during the time period of the scan. The situation changes after the other side of the zinc square is reached for $X = 2260$ μm, and the concentration values derived from the potential recording at the ISME returns to those found at the beginning of the scan line. And the situation remains almost constant until the end of the probe travel.

Quantitative determinations of the concentration of Zn^{2+} ions in the system are attained in all the subsequent line scans plotted in Figure 3A. They all show a clear accumulation of metal ions above the zinc strip, which quickly fades away as the probe moves on the resin sleeve to greater distances from the metal. This is already the case for the line scan measured after 13 min, which shows the progressive enrichment of the electrolyte in metal ions above the zinc strip during the duration of the probe travel as well. This feature is not observed in the scan lines measured for longer exposures, because the higher metal concentrations existing at those times are not significantly modified by the metal fluxes leaving the corroding surface below. The concentration of metal ions continue to increase with the elapse of time until about 30 min after immersion, and a stationary is observed for the rest of the experiment duration. This behaviour is more clearly observed by inspection of Figure 4, which gives the maximum metal ion concentration obtained from each line scan, thus effectively plotting the variation of Zn^{2+} concentration with exposure time. It is interesting to notice the development of a maximum concentration of metal ions after ca. 30 min, and the concentration remains practically unchanged for the remaining of the experiment. Since it is unlikely that the corrosion process might have stopped after this short exposure when the metal is galvanically coupled to iron in 10 mM NaCl aqueous solution, the attainment of a maximum concentration for Zn^{2+} ions in the electrolyte must be due to

6

the onset of metal precipitation through reaction [48]:

$$Zn^{2+} + nH_2O \rightarrow [Zn(OH)_n]^{(2-n)} + nH^+, \quad pK_1 = 7.96 \tag{1}$$
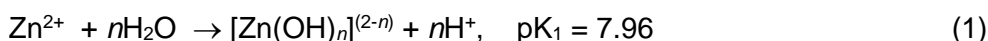
Accordingly, the local pH of the electrolyte in contact with the surface of zinc should be ca. 3.9, a value that agrees well with the pH values observed for the same system when a pH-sensitive antimony electrode was employed as the SECM tip instead [40].

Another feature is that the greater change in metal ion concentrations when departing from the corroding sample occurs within a short distance from the metal limit (in excess of two decades in the values of pZn), which is followed by a rather slow asymptotic decay to the values characteristic of the bulk electrolyte for the furthest distance covered in this experiment. All these observations are consistent with previous studies based on the measurement of ionic fluxes in the electrolyte adjacent to the same zinc-iron galvanic system made by SVET [29].

The behaviour of the novel solid contact Zn^{2+} ISME was compared with that exhibited by conventional micropipette electrodes by conducting a similar set of experiments on the same experimental system. Figure 3B shows a selection of the line scans recorded after different exposures. In this case, the ion-selective electrode does not provide data with enough stability and reproducibility to record quantitative data in potentiometric SECM. The plots exhibit big oscillations, and they are greatly affected by the scan direction for this scan rate, whereas the solid contact ISME did not show these limitations. In this way, the superiority of a solid contact ISME for the potentiometric operation of the SECM could be established.

The distribution of Zn^{2+} species in the electrolyte phase over a corroding sample could also be monitored as a function of the distance from the surface. In this case, the ISME probe moved over the specimen until it was placed approximately above the centre of the Zn sample, and subsequently retracted from the surface by means of the Z positioner. Figure 5 depicts the corresponding plot measured whereas the ISME was moved from the distance of closest approach in our work (i.e. 25 μm) until a distance of 1200 μm. The concentration of Zn^{2+} ions diminished steadily during this operation. The stability of the microsensor is further evidenced by switching the scan direction in order to measure the corresponding approach curve. Both plots are well superimposed, a further evidence of a robust and stable potentiometric probe. Thus, the distribution of metal ions can be imaged by scanning in the XZ plane as it is shown in Figure 6. This image is effectively a composition of scan lines recorded in the X direction in a movement parallel to the surface of the sample. In this way, each scan line extends for

2500 μm. Once the scan line has been completed, the probe is retracted on the Z axis to a new height, and the next scan line was recorded. In order to reduce the time required to acquire a complete map up to a distance of 1000 μm, well inside the bulk of the electrolyte. That is, scan lines have been recorded only at a selection of probe-surface distances, and the composed map given in Figure 6 shows some blank lines accordingly. Yet, the concentration profiles in both the X and Z directions can be clearly deduced from the observation of this image.

4. Conclusions

This study reveals that solid contact Zn^{2+} ion sensor microelectrodes can be used to monitor concentration distribution of corrosion products in a corroding system with the scanning electrochemical microscope operating using rastering conditions similar to those employed with the amperometric modes.

The formation of zinc soluble species is identified in the anodic zone covering the zinc strip coupled to iron when exposed to an aqueous 10 mM NaCl solution. The time evolution of the corroding system could thus be monitored.

SECM images depicting the concentration distribution of Zn^{2+} species over the reactive system can be obtained by recording scan lines in the XY plane parallel to the investigated surface, or as depth profiles when the XZ plane (i.e. perpendicular to the surface) is taken instead.

Summarizing, this work demonstrates the complementary use of the potentiometric operation of the scanning electrochemical microscope to detect local changes of the ion activity as result of corrosion reactions.

References:

1. S.E. Pust, W. Maier, G. Wittstock, Investigation of localized catalytic and electrocatalytic processes and corrosion reactions with scanning electrochemical microscopy (SECM), Z. Phys. Chem. 222 (2008) 1463–1517.

2. L. Niu, Y. Yin, W. Guo, M. Lu, R. Qin, S. Chen, Application of scanning electrochemical microscope in the study of corrosion of metals, J. Mater. Sci. 44 (2009) 4511–4521.

3. Y. González-García, J.J. Santana, J. González-Guzmán, J. Izquierdo, S. González, R.M. Souto, Scanning electrochemical microscopy for the investigation of localized degradation processes in coated metals, Prog. Org. Coat. 69 (2010) 110-117.

4. R.M. Souto, S. Lamaka, S. González, Uses of scanning electrochemical microscopy in corrosion research, in: A. Méndez-Vilas, J. Díaz (Eds.), Microscopy: Science, technology, applications and education, Vol. 3; Formatex Research Center, Badajoz (Spain), 2010, pp. 2162-2173.

5. N. Casillas, S. Charlebois, W.H. Smyrl, H.S. White, Pitting corrosion of titanium, J. Electrochem. Soc. 141 (1994) 636-642.

6. S.B. Basame, H.S. White, Scanning electrochemical microscopy of native titanium oxide films. Mapping the potential dependence of spatially-localized electrochemical reactions, J. Phys. Chem. 99 (1995) 16430-16435.

7. Y.Y. Zhu, D.E. Williams, Scanning Electrochemical microscopic observation of a precursor state to pitting corrosion of stainless steel, J. Electrochem. Soc. 144 (1997) L43-L45.

8. Y. González-García, G.T. Burstein, S. González, R.M. Souto, Imaging metastable pits on austenitic stainless steel *in situ* at the open-circuit corrosion potential, Electrochem. Commun. 6 (2004) 637-642.

9. K. Mansikkamäki, P. Ahonen, G. Fabricius, L. Murtomäki, K. Kontturi, Inhibitive effect of benzotriazole on copper surfaces studied by SECM, J. Electrochem. Soc. 152 (2005) B12-B16.

10. S. Hocevar, S. Daniele, C. Bragato, B. Ogorevic, Reactivity at the film/solution interface of ex situ prepared bismuth film electrodes: A scanning electrochemical

microscopy (SECM) and atomic force microscopy (AFM) investigation, Electrochim. Acta 53 (2007) 555-560.

11. D. Battistel, S. Daniele, R. Gerbasi, M.A. Baldo, Characterization of metal-supported Al_2O_3 thin films by scanning electrochemical microscopy, Thin Solid Films 518 (2010) 3625-3631.

12. J. Izquierdo, J.J. Santana, S. González, R.M. Souto, Uses of scanning electrochemical microscopy for the characterization of thin inhibitor films on reactive metals: the protection of copper surfaces by benzotriazole, Electrochim. Acta 55 (2010) 8791-8800.

13. R.M. Souto, Y. González-García, S. González, G.T. Burstein, Damage to paint coatings caused by electrolyte immersion as observed in situ by scanning electrochemical microscopy, Corros. Sci. 46 (2004) 2621-2628.

14. A.C. Bastos, A.M. Simões, S. González, Y. González-García, R.M. Souto, Application of the scanning electrochemical microscope to the examination of organic coatings on metallic substrates, Prog. Org. Coat. 53 (2005) 177–182.

15. R.M. Souto, Y. González-García, S. González, *In Situ* monitoring of electroactive species by using the scanning electrochemical microscope. Application to the investigation of degradation processes at defective coated metals, Corros. Sci. 47 (2005) 3312-3323.

16. A.M. Simoes, D. Battocchi, D.E. Tallman, G.P. Bierwagen, SVET and SECM imaging of cathodic protection of aluminium by a Mg-rich coating, Corros. Sci. 49 (2007) 3838-3849.

17. R.M. Souto, Y. González-García, S. González, Evaluation of the corrosion performance of coil-coated steel sheet as studied by scanning electrochemical microscopy, Corros. Sci. 50 (2008) 1637-1643.

18. R.M. Souto, Y. González-García, S. González, Characterization of coating systems by scanning electrochemical microscopy: surface topology and blistering, Prog. Org. Coat. 65 (2009) 435–439.

19. R.M. Souto, Y. González-García, S. González, G.T. Burstein, Imaging the origins of coating degradation and blistering caused by electrolyte immersion assisted by SECM, Electroanalysis 21 (2009) 2569-2574.

20. R.M. Souto, L. Fernández-Mérida, S. González, SECM imaging of interfacial processes in defective organic coatings applied on metallic substrates using oxygen as redox mediator, Electroanalysis 21 (2009) 2640-2646.

21. E. Salamifar, M.A. Mehrgardi, M.F. Mousavi, Ion transport and degradation studies of a polyaniline-modified electrode using SECM, Electrochim. Acta 54 (2009) 4638–4646.

22. R.M. Souto, Y. González-García, J. Izquierdo, S. González, Examination of organic coatings on metallic substrates by scanning electrochemical microscopy in feedback mode: revealing the early stages of coating breakdown in corrosive environments, Corros. Sci. 52 (2010) 748-753.

23. J.J. Santana, J. González-Guzmán, J. Izquierdo, S. González, R.M. Souto, Sensing electrochemical activity in polymer coated metals during the early stages of coating degradation by means of the scanning vibrating electrode technique, Corros. Sci. 52 (2010) 3924-3931.

24. J.J. Santana, J. González-Guzmán, L. Fernández-Mérida, S. González, R.M. Souto, Visualization of local degradation processes in coated metals by means of scanning electrochemical microscopy in the redox competition mode, Electrochim. Acta 55 (2010) 4488-4494.

25. C.H. Paik, H.S. White, R.C. Alkire, Scanning electrochemical microscopy detection of dissolved sulfur species from inclusions in stainless steel, J. Electrochem. Soc. 147 (2000) 4120-4124.

26. C.H. Paik, R.C. Alkire, Role of sulfide inclusions on localized corrosion of Ni200 in NaCl solutions, J. Electrochem. Soc. 148 (2001) B276-B281.

27. K. Fushimi, M. Seo, An SECM observation of dissolution distribution of ferrous or ferric ion from a polycrystalline iron electrode, Electrochim. Acta 47 (2001) 121-127.

28. A.C. Bastos, A.M. Simões, S. González, Y. González-García, R.M. Souto, Imaging concentration profiles of redox-active species in open-circuit corrosion processes with the scanning electrochemical microscope, Electrochem. Commun. 6 (2004) 1212-1215.

29. A.M. Simões, A.C. Bastos, M.G. Ferreira, Y. González-García, S. González, R.M. Souto, Use of SVET and SECM to study the galvanic corrosion of an iron-zinc cell, Corros. Sci. 49 (2007) 726-739.

30. S. Modiano, J.A.V. Carreño, C.S. Fugivara, R.M. Torresi, V. Vivier, A.V. Benedetti, O.R. Mattos, Changes on iron electrode surface during hydrogen permeation in borate buffer solution, Electrochim. Acta 53 (2008) 3670-3679.

31. S. González, J.J. Santana, L. Fernández-Mérida, R.M. Souto, Sensing electrochemical activity in polymer coated metals during the early stages of coating degradation – Effect of the polarization of the substrate, Electrochim. Acta 56 (2011) doi: 10.1016/j.electacta.2011.03.077.

32. B. Horrocks, M.V. Mirkin, D.T. Pierce, A.J. Bard, G. Nagy, K. Toth, Scanning electrochemical microscopy. 19. Ion-selective potentiometric microscopy. Anal. Chem. 65 (1993) 1213-1224.

33. G. Nagy, L. Nagy, Scanning electrochemical microscopy: a new way of making electrochemical experiments, Fresenius J. Anal. Chem. 366 (2000) 735–744.

34. G. Denuault, G. Nagy, K. Tóth, Potentiometric probes, in: A.J. Bard, M.V. Mirkin (Eds.), Scanning electrochemical microscopy; Marcel Dekker, New York, 2001, pp. 397-444.

35. G. Nagy, L. Nagy, Electrochemical sensors developed for gathering microscale chemical information, Anal. Lett. 40 (2007) 3–38.

36. S. González, J.J. Santana, Y. González-García, L. Fernández-Mérida, R.M. Souto, Scanning electrochemical microscopy for the investigation of localized degradation processes in coated metals: Effect of oxygen, Corros. Sci. 53 (2011) 1910-1915.

37. R.M. Souto, Y. González-García, D. Battistel, S. Daniele, In situ SECM detection of metal dissolution during zinc corrosion by means of mercury sphere-cap microelectrode tips, J. Phys. Chem. C (2011) submitted.

38. D.O. Wipf, F. Ge, T.W. Spaine, J.E. Baur, Microscopic measurement of pH with iridium oxide microelectrodes, Anal. Chem. 72 (2000) 4921-4927.

39. E. Klusmann, J.W. Schultze, pH-Microscopy: technical application in phosphating solutions, Electrochim. Acta 48 (2003) 3325-3332.

40. J. Izquierdo, L. Nagy, Á. Varga, J.J. Santana, G. Nagy, R.M. Souto, Spatially-resolved measurement of electrochemical activity and pH distributions in corrosion processes by scanning electrochemical microscopy using antimony microelectrode tips, Electrochim. Acta (2011) submitted.

41. G. Gyetvai, S. Sundblom, L. Nagy, A. Ivaska, G. Nagy, Solid contact micropipette ion selective electrode for potentiometric SECM, Electroanalysis 19 (2007) 1116–1122.

42. G. Gyetvai, L. Nagy, A. Ivaska, I. Hernadi, G. Nagy, Solid Contact Micropipette Ion Selective Electrode II: Potassium Electrode for SECM and In Vivo Applications, Electroanalysis 21 (2009) 1970-1976.

43. Á. Varga, L. Nagy, J. Izquierdo, I. Bitter, R.M. Souto, G. Nagy, Development of solid contact micropipette Zn-ion selective electrode for corrosion studies, Anal. Lett. 43 (2011) in press.

44. E. Lindner E., M. Horváth, K. Tóth, E. Pungor, I. Bitter, B. Ágai, L. Tõke, Zinc selective ionophores for potentiometric and optical sensors, Anal. Lett. 25 (1992) 453-470.

45. R.C. Thomas, Ion-selective intracellular microelectrodes: How to make and use them; Academic Press, London, 1978.

46. D. Ammann, Ion-selective microelectrodes. Principles, design and application, Springer-Verlag, Berlin, 1986.

47. B. Kovács, B. Csóka, G. Nagy, I. Kapui, R.E. Gyurcsányi, K. Tóth, Automatic target location strategy - A novel approach in scanning electrochemical microscopy, Electroanalysis 11 (1999) 349-355.

48. Y.Y. Lur'e, Handbook of Analytical Chemistry (In Russian, Spravochnik po Analiticheskoi Himii), 6th ed., Himiya, Moscow, 1989.
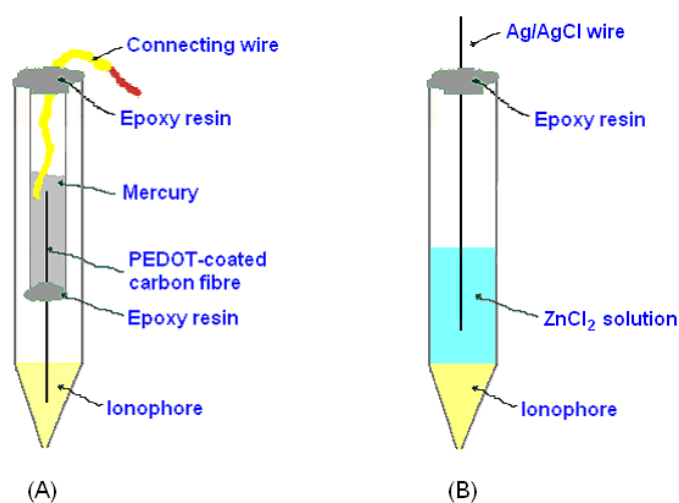
Figure 1. Sketches of the two configurations of Zn^{2+}-ISMEs employed in the experiments: (A) solid contact, and (B) conventional liquid contact. The diameter of the pipette tips used in the studies ranged between 10-50 µm.
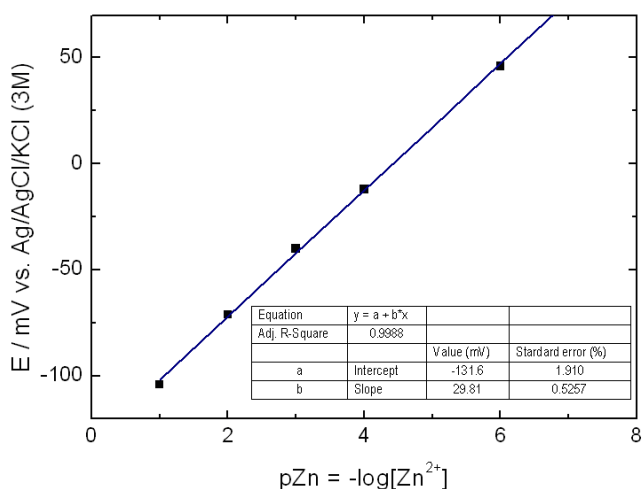

Figure 2. Calibration plot determined from the potentiometric response of the solid contact Zn^{2+}-ion selective microelectrode to solutions of varying Zn^{2+} concentration.
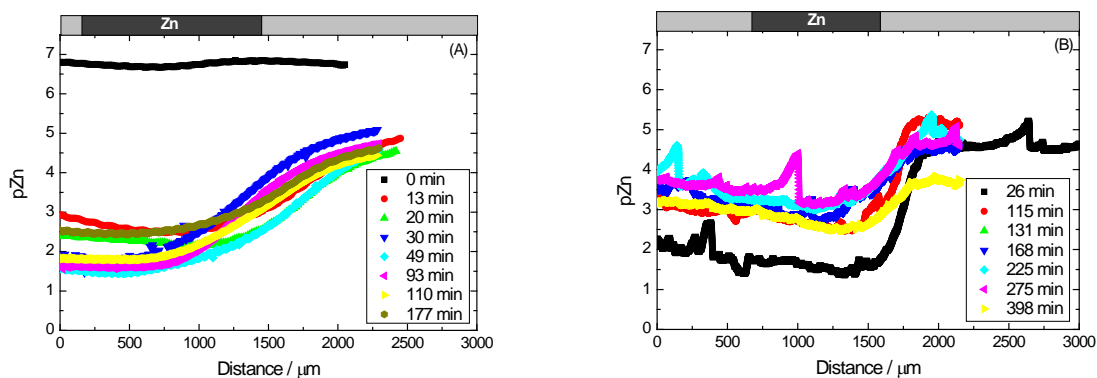
13

Figure 3. Potentiometric SECM scan lines measured above the zinc specimen in a zinc-iron galvanic pair immersed in 10 mM NaCl after different times as indicated in the plots. Two different Zn^{2+}-ISMEs were employed as SECM tips, namely: (A) the novel solid-contact micropipette system described in this work, and (B) a conventional micropipette ISME having a liquid contact. Vertical tip - surface distance: 25 μm.
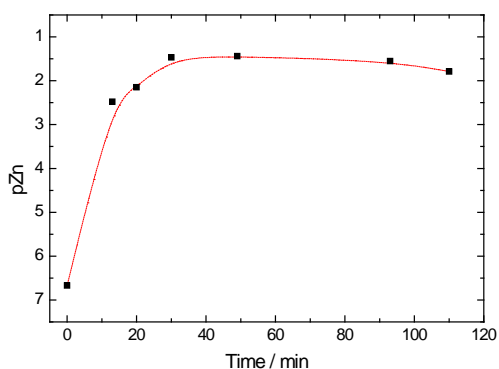

Figure 4. Time evolution of the Zn^{2+} concentration measured above the zinc specimen from the potentiometric scan lines depicted in Figure 3A.
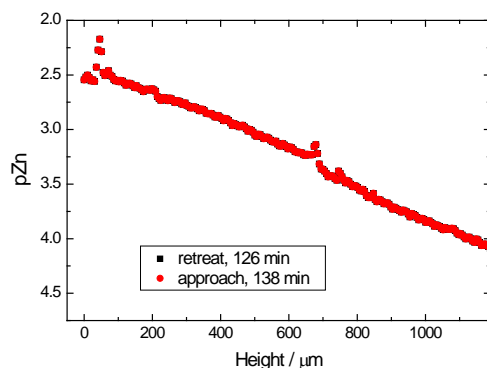

Figure 5. Distribution of Zn^{2+} ion concentration above the zinc specimen measured with the solid contact Zn^{2+}-ISME as the height of the tip is changed. The zinc-iron galvanic pair has been immersed in 0.1 M NaCl for the immersion times given in the graphs. The approach and retreat lines closely match each other.
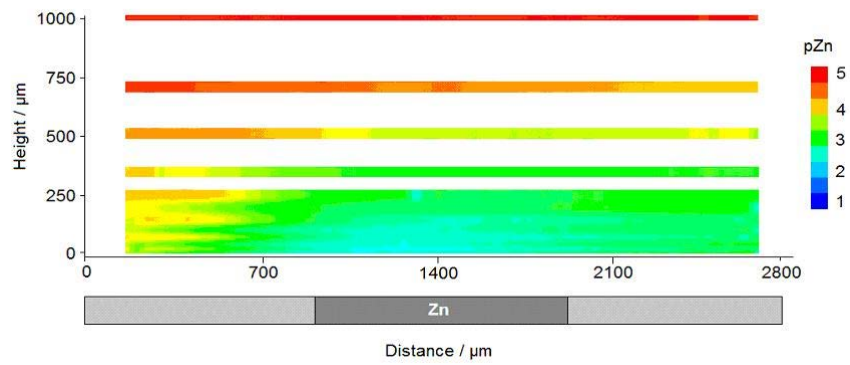
14

Figure 6. Distribution of Zn^{2+} ion concentration in a plane perpendicular to the surface of the zinc specimen registered after the iron-zinc pair has been immersed in 10 mM NaCl for 5 hours.